LAMINAR-TO-TURBULENT FLOW TRANSITION IN MICROCHANNELS

Gian Luca Morini

Dipartimento di Ingegneria – Università degli Studi di Ferrara

Via Saragat 1, 44100 Ferrara, ITALY

ABSTRACT

Some experimental results on heat transfer and pressure drop through microchannels evidenced that the classical theory, validated for large sized channels, could be not valid for channels having an hydraulic diameter smaller than 1 mm. Also the transition from laminar to turbulent regime is found to happen to Reynolds numbers lower than those expected and this fact is considered a confirmation of the disagreement with the classical theory. In this paper is shown as many experimental results on the transition from laminar to turbulent flow in microchannels can be explained by using the "Obot-Jones model" obtained by means of the classical theory for conventional sized channels.

Dr. Gian Luca Morini

Dipartimento di Ingegneria – Università degli Studi di Ferrara

Via Saragat 1, 44100 Ferrara (Italy)

Tel. ++39 0532 293825

Fax ++39 0532 768602

e-mail: glmorini@ing.unife.it

The development of micro-fluidic devices has been particularly striking during the past 10 years. Today, the research on MEMS (Micro-Electro-Mechanical Systems) is exploring different applications which involve the dynamics of fluids and the single and two-phase forced convective heat transfer in microchannels. Recent advances in micro-fabrication techniques permit to build microchannels with small hydraulic diameters (1000-1 μm), in different ways. As example, the microchannels can be produced directly by chemical etching on silicon wafers; in this case, the shape of the channels depends on a variety of factors such as the crystallographic nature of the silicon used. When a KOH anisotropic etching technique is employed, it is possible to obtain microchannels having a fixed cross-section depending on the orientation of the silicon crystal planes; for instance, the microchannels etched in <100> or in <110> silicon, will have a trapezoidal cross-section (with an apex angle of 54.74° imposed by the crystallographic morphology of the silicon) or a rectangular cross-section respectively. In the present paper, KOH-etched microchannels having cross-sections trapezoidal, hexagonal (obtained gluing together two trapezoidal channels) and rectangular will be considered (see Fig. 1).

An interesting aspect of fluid dynamics through microchannels is lied to the transition from laminar to turbulent regime. Recent reviews of the literature on this topic are due to Bowman and Maynes [1] and Obot [2]. Some studies indicate that the transition from laminar to turbulent flow in micro-scale passages takes place at critical Reynolds number ranging from 300 to 2000. In particular, the experimental data of Wu and Little [3,4] on glass and silicon microchannels having an hydraulic diameter between 45.5 μm and 83.1 μm, observed that for Re<1000 the flow is laminar and for Re>3000 the flow is fully turbulent. Choi *et al.* [5], analyzing microtubes with an hydraulic diameter of 53 μm and 81.2 μm, indicated that the transition to turbulent flow occurs at Re=2000. They found that this value decreases for smaller microchannels (Re=500 for D_h=9.7

μm and 6.9 μm). This fact is not coherent with the indication of the classical theory for large sized tubes. The experimental analysis of metallic microchannels conducted by Wang and Peng [6] and successively by Peng *et al.* [7-8] indicated that the transition through rectangular microchannels could be early with respect the Reynolds numbers found by Wu and Little [3,4]. In particular, Wang and Peng [6] and Peng and Peterson [7] studied the laminar-to-turbulent transition by heating rectangular microchannels deep 700 μm and having a width between 800 and 200 μm and by observing the trend of the convective heat transfer coefficient. For water or methanol, they found that the transition region drops to Reynolds numbers ranging from 300-400 to 1000. Successively, Peng and Peterson [8] studied the forced convection of binary water-methanol mixture through rectangular microchannels, wide 100-400 μm and deep 200-300 μm; their experimental data indicated that the laminar heat transfer regime ceases at a lower Reynolds numbers of 70-400 and that fully turbulent regime is achieved at Reynolds numbers of 200-700. Obot [2], analyzing critically the experimental results cited above, arrives to the conclusion that there is not strong experimental evidence to support the existence of transitional or turbulent flow for Reynolds number less than 1000. Recently, Celata *et al.* [9] studied the laminar-to-turbulent flow transition in a microtube having an hydraulic diameter of 130 μm. They stressed the role of the relative roughness on the transition. Their experimental data are in good agreement with the flow transition prediction for rough commercial tubes. In this paper the "Obot-Jones method" for conventional sized channels will be used in order to predict the range of Reynolds numbers that corresponds to the transition from laminar to turbulent regime through non-circular microchannels. The role of the cross-section geometry, of the microchannel aspect ratio and of the relative roughness on the laminar-to-turbulent flow transition will be evidenced.

THE "OBOT-JONES MODEL"

Jones [10] noted that, for non-circular ducts, at constant Reynolds number based on hydraulic diameter, the friction factor increases monotonically with increasing the aspect ratio. He concluded that the hydraulic diameter is not the proper length dimension to use in the Reynolds number definition to insure similarity between the circular and non-circular ducts. For this reason, Jones introduced a modified characteristic length (named "laminar equivalent" diameter) defined as follows:

$$D_L = \Phi_g^*(g) D_h \tag{1}$$

where the function Φ_g* depends on the geometry of the channel cross-section only. It means that, for a rectangular, trapezoidal or double-trapezoidal microchannel, the function Φ_g* depends, for each cross-section (g), on the aspect ratio γ=b/a (see Fig. 1). As demonstrated for rectangular duct by Jones [10], for fixed geometry of the channel, it is possible to calculate Φ_g* by means of the fully developed Poiseuille number for laminar regime. Obot [11] developed the Critical Friction Method (CFM) in order to reduce the friction data for non-circular passages on the classical circular tube relations. The CFM indicated that Φ_g* is related to the ratio between the critical Reynolds number for tubes ($Re_{c,c}$) and non-circular ducts ($Re_{g,c}$). By using this method, the determination of the value of the critical Reynolds number for a microchannel having a cross-section of fixed geometry, can be calculated by means of the following equation:

$$\mathrm{Re}_{g,c} = \frac{\mathrm{Re}_{c,c}}{f_g^*} \tag{2}$$

Eq.(2) underlines how, for non-circular channels, the transition between the laminar and turbulent flow could happen for Reynolds numbers less than those for circular ducts (if Φ* greater than 1).

In order to calculate the value assumed by Φ_g* for trapezoidal, double trapezoidal and rectangular

microchannels, a 2D analysis of the flow field is made under the following assumptions:

- the transport processes are considered to be steady-state and bi-dimensional;
- the fluid is Newtonian, incompressible, isothermal and with a laminar fully developed profile of velocity;
- all the channel walls are rigid and non-porous;
- the fluid physical properties are considered as constant.

Under the mentioned hypotheses the fluid momentum equation can be written as follows:

$$\nabla^{*2} \mathrm{V} = -\mathrm{p}^{*} \tag{3}$$

where the following dimensionless quantities are used:

$$\Omega^{*} = \frac{\Omega}{D_h^2}; \quad \Gamma^{*} = \frac{\Gamma}{D_h}; \quad \nabla^{*} = D_h \nabla; \quad V(x,y) = \frac{u}{W}; \quad p^{*} = -\frac{D_h^2}{mW}\frac{dp}{dz}; \tag{4}$$

Ω denotes the area of the cross-section, Γ the perimeter, W the average velocity and D_h the hydraulic diameter of the microchannel.

The momentum equation (Eq.(3)) is solved by using the boundary condition of no-slip at the wall; it means that in the present analysis the rarefaction effects are neglected. For liquids, this assumption is justified because the typical hydraulic diameters of a micro-device are of the order of 1-1000 μm whereas the molecular mean free path, under ambient conditions, is of the order of 0.1-1 nm; as consequence, the Knudsen number ($Kn=\lambda/D_h$) is always less than 0.001.

The problem described by Eq.(3) has been solved numerically by means of a self-made numerical code written, by using the Finite Element Method, for a generic microchannel having a trapezoidal (ϕ=54.74°), rectangular (ϕ=90°) or hexagonal (double trapezoidal) cross-section. In this manner, the velocity distribution through the microchannel has been determined. From the velocity distribution it is possible to derive the value assumed by the main flow parameters as

function of the microchannel geometry. For the aim of the present analysis, the Poiseuille number, defined as the product of the Fanning friction factor for fully developed flow (*f*) and the Reynolds number (*Re*), is determined. The Poiseuille number can be calculated by the velocity field by means of the following relation:

$$(f\,\mathrm{Re})_{fd} = \frac{2\bar{t}_W D_h}{mW} = -\frac{1}{2\Omega^*}\int_{\Gamma^*} n\cdot\nabla^* V\, d\Gamma^* = \frac{p^*}{2} \tag{5}$$

The Eq.(5) underlines that the Poiseuille number in laminar regime depends on the cross-section geometry only. Finally, as demonstrated for rectangular duct by Jones [10] and confirmed by Obot [11] for non-circular channels, it is possible to calculate the Φ_g* function by means of the following equation:

$$\Phi_g^* = \frac{16}{(\mathrm{f\,Re_{fd}})_g} \tag{6}$$

The accuracy of the numerical results has been tested comparing the Poiseulle numbers with the values quoted in literature.

For rectangular channel, the comparison between the results of this work and the analytical results quoted by Shah and London [12] is shown in Table 1. It is possible to verify that the agreement is very good; this fact validates the numerical procedure followed in this work.

In Table 2 are quoted, as function of the aspect ratio of the channel, the numerical values obtained for the Poiseuille number in the case of a trapezoidal and double trapezoidal KOH-etched microchannels. In literature two different definition of aspect ratio are used for trapezoidal channels; Shah and London [12] use β defined as ratio between the height (b) and the mimimum width (*c*) of the channel, instead Sadasivam *et al.* [13] use γ defined as ratio between the height (*b*) and the maximum width (*a*) of the channel. In Table 2, both β and γ are quoted in order to simplify the use of the data.

For the trapezoidal microchannels, the aspect ratio γ cannot exceed the value of $tg(\phi)/2$ (equal to 0.707 for ϕ=54.74°) corresponding to the degeneration of the cross-section to the triangular geometry ($\beta=\infty$). In the case of double trapezoidal cross section, the aspect ratio γ ranges between 0 (parallel plates) and 1.414 (rhombic configuration). Richter *et al*. [14] summarized the geometry coefficients C_R (where $C_R=(fRe)_{fd}\,\Gamma^*/2$) for typical cross sections occurring in silicon micro-devices. Urbanek *et al.* [15] found that the geometry coefficient C_R is 35.12 for the KOH-etched triangle (γ=0.707); in the present analysis the calculated value of C_R is 35.118. Ulrich (cited in the work of Richter *et al.* [14]) proposed a simple correlation in order to calculate the value of C_R for KOH-etched trapezoidal microchannels:

$$C_R = \frac{12 - 1.38a + 4a^2}{a - 0.85a^2 + 0.28a^3} \quad with \quad a = \frac{1}{\frac{1}{g} - \frac{1}{tg\,f}} \tag{7}$$

In Fig. 2 the results obtained in the present analysis for trapezoidal microchannels are compared with the Ulrich's correlation; it is possible to note the good agreement between the present results and Eq.(7); the maximum difference is equal to 1.5%.

For isosceles triangular ducts, Migay [16] obtained a closed-form equation for Poiseuille number by point-maching, discrete least squares method. Takuto *et al*. [17] quoted the values of fRe_{fd} for KOH-etched triangle and for trapezoidal microchannels fabricated on <100> silicon with γ equal to 0.134 and 0.051. Urbanek *et al*. [15] obtained numerically the value of the Poiseuille number for a trapezoidal channel with an aspect ratio γ of 0.027. The results of Migay [16], Takuto *et al.* [17] and Urbanek *et al*. [15] are in agreement with the numerical values obtained in the present work, as shown in Table 3.

Recently Damean and Regtien [18] presented fully developed Poiseuille numbers for laminar flow through hexagonal ducts etched in <100> silicon. By using a commercial software package

dedicated for fluid flow simulations, they calculated the variation of the Poiseuille number with the aspect ratio of a double trapezoidal microchannel. They derived a polynomial approximation of the dependence of fRe_{fd} on the microchannel aspect ratio. In Fig. 3 the data quoted in Table 2 are compared with the prediction of the fRe_{fd} obtained by using the correlation proposed by Damean and Regtien [18]. The agreement between the present results and the correlation of Damean and Regtien is good; the maximum difference is equal to 0.83 %, for aspect ratios ranging between 0 and 1.414.

A fifth order polynomial approximation for calculating $(fRe)_{fd}$ as function of the channel aspect ratio (γ) is given with the aim of offering a very simple but accurate tool for technicians and designers involved in microfluidic applications:

$$f\,\mathrm{Re}_{fd} = \sum_{i=0}^{5} g_i \gamma^i \tag{8}$$

The values of the constants g_i are listed in Table 4; the maximum relative difference (Δ) is positive when the Eq.(8) gives values greater than the rigorous calculation. The correlations proposed in this paper for trapezoidal and double-trapezoidal channels are more accurate than those of Ulrich [14] and Damean and Regtien [18].

PREDICTIONS OF THE MODEL

The polynomial approximation of the Poiseuille number furnished by Eq.(8), in addition with Eq.(6), permits to calculate the value of Φ_g^* for all the cross-sections considered. In Fig. 4 the value of Φ_g^* is quoted for rectangular, trapezoidal and double-trapezoidal KOH-etched microchannels as function of the aspect ratio (γ=b/a).

It is possible to note that Φ_g^* is less than 1 for $\gamma<0.268$ for trapezoidal channels, for $\gamma<0.489$ for

hexagonal channels and for $\gamma<0.441$ (or $\gamma>2.268$) for rectangular channels.

Typically, in the Moody chart for commercial tubes, three characteristics zones (laminar, transition and turbulent regimes) can be distinguished; the end of the laminar zone and the onset of the fully developed turbulent regime are individuated with a minimum and a maximum of the friction factor respectively. Two critical Reynolds numbers define the boundaries of the transition region. Idelchick [19] quoted the following correlations in order to calculate the limits of the transition region for isothermal flow through a commercial tube with non-uniform roughness:

$$\mathrm{Re}_{c,1} = 1160\left(\frac{e}{D_h}\right)^{-0.11} \qquad \mathrm{Re}_{c,2} = 2090\left(\frac{e}{D_h}\right)^{-0.0635} \tag{9}$$

where ε is the absolute roughness.

In addition, Idelchick [19] underlined that in laminar regime, for rough tubes, there is a departure of the friction factor from the classical Haghen-Poiseuille law before the transition region. This effect could be enhanced for flows through microchannels because, at the same Reynolds number, the average velocity is higher in a channel having a small hydraulic diameter. The onset of the departure can be predicted by means of the following correlation [19]:

$$\mathrm{Re}_{c,o} = 754\exp\left(\frac{0.0065}{e/D_h}\right) \tag{10}$$

valid for $\varepsilon/D_h>0.007$.

In this paper, for smooth channels a value of ε/D_h equal to 0.007 is assumed; it means that one supposes the roughness of a smooth microchannel of the order of nanometers. At this point, the critical Reynolds numbers $\mathrm{Re}_{c,o}$, $\mathrm{Re}_{c,1}$ and $\mathrm{Re}_{c,2}$ can be calculated in order to predict the transition region for smooth and rough microchannels for any value of the aspect ratio and for any cross-section. In Table 5a and 5b the values of the three critical Reynolds numbers defined by Eqs.(9)-

(10) for smooth and rough (ε/D_h=0.02) microchannels are quoted respectively.

Comparing the results quoted in Table 5a and Table 5b, it is evident the role of the roughness and of the aspect ratio of the cross section on the transition between laminar and turbulent regime. For fixed geometry, the transition comes early if the roughness increases. In addition, for fixed roughness, the transition comes early if the cross section tends to the square (for rectangular geometry) or to the triangle (for trapezoidal geometry) or to the rhomb (for double-trapezoidal geometry).

VALIDATION OF THE MODEL

In the experimental works of Wu and Little [3,4] some microchannels of silicon and glass are tested. The glass channels present a rectangular cross section with two rounded corner and with an high value of relative roughness (ε/D=0.2-0.3) displaced non uniformly along the wetted perimeter. The silicon microchannels are realized with a photolitographic technique on a <100> silicon wafer; in this case the channels are trapezoidal and can be considered smooth. Comparing the results of Wu and Little [3,4] for glass and silicon channels, is well evident the role of the relative roughness in order to come early the transition. In order to test the model presented in this paper, the data of the silicon microchannel named S(3) are considered (smooth channel). Wu and Little concluded that the transition occurs at Reynolds numbers ranging from 1000 to 3000. It is possible to see in Table 6 that the critical Reynolds numbers calculated by means of the model presented in this paper are quite in accordance with the experimental observations of Wu and Little.

Acosta *et al.* [20] presented friction factors for rectangular microchannels with an hydraulic diameter ranging between 368.9 μm and 990.4 μm. The rectangular channels investigated have a very small value of the aspect ratio ($0.019<\gamma<0.05$). The microchannels evidenced very similar

values of the friction factors; this fact is consistent with the asymptotic behaviour of the Poiseuille number (fRe_{fd}) for small or large aspect ratio. In Table 6 the value of the critical Reynolds number found by Acosta *et al.* is compared with the prevision obtained by using the model proposed; also in this case the agreement is good.

Gui and Scaringe [21] measured experimentally the friction factors for water through trapezoidal microchannels having 1 mm of width and with channel depths ranging between 79 and 325 μm (aspect ratio γ between 0.079 and 0.325). The roughness of the channels was not measured but they suggested a value of ε/D_h equal to 0.015. The critical Reynolds number found experimentally is 1400 for γ equal to 0.079. In Table 6 are quoted the values of the critical Reynolds numbers predicted with the model; the agreement is good.

Harms *et al.* [22] investigated the developing convective heat transfer in rectangular microchannels fabricated in a 2 mm thick <110> silicon substrate by means of chemical etching. Two different channels with an aspect ratio equal to 0.04 and 0.244 were tested and the critical Reynolds number is experimentally determined. The accordance with the predictions of the model is good for the channel having γ equal to 0.244. For the deep rectangular microchannel with γ equal to 0.04 the model furnishes critical Reynolds numbers higher than the experimental one. This behaviour could be due to the effect of the variation of the thermophysical properties with the temperature. In fact, the channel having γ=0.04 has an hydraulic diameter of 1923 μm instead of 404 μm of the channel having γ=0.244; because higher hydraulic diameters determine higher thermal resistance, the variation of the temperature is higher in the deep channel.

Ding *et al.* [23] performed an experimental work to investigate the pressure drop for R134a and R12 through microchannels with triangular and rectangular cross section. In Table 6, a comparison between the model and their experimental results is quoted for two square

microchannels with an hydraulic diameter of 400 μm and 600 μm. An interesting particularity of these experimental results is that the role of the relative roughness in order to anticipate the transition appears not confirmed.

Jiang *et al.* [24] tested a micro heat exchanger with microchannels fabricated from 0.7 mm thick pure copper plates on a wire cutting machine. The channels are rectangular and have an hydraulic diameters of 300 μm. Measurements with electron microscope showed that the surface roughness of the microchannels was from 5.8 to 36.3 μm; it means an average relative roughness of the microchannels of 0.1. In addition, due to microfabrication technique utilised, the cross-section of the microchannels is not perfectly rectangular. They found that the transition from laminar to turbulent flow occurs much earlier (Re=600) and the fully developed turbulent regime is present for Re>2800; it is possible to see in Table 6 that the predictions of the model are quite in accordance also with the results of Jiang *et al.* [24].

Wang and Peng [6], analysed the single-phase forced flow convection of water or methanol through rectangular microchannels machined in parallel on a stainless steel plate. In this experiment, the laminar-to-turbulent flow transition is induced by or associated with variations in the liquid thermophysical properties due to the increases of the temperature and it occurs in the range of 300-800 of the Reynolds number. It is particularly important to underline that the Reynolds number can be doubled over the heated length of the microchannels. In addition, there is not information about the roughness of microchannels tested.

Peng and Peterson [8] quoted the transition Reynolds numbers for different aspect ratio of rectangular microchannels for water and methanol flows. The tested metallic microchannels are similar to the microchannels utilised by Jiang *et al.* [24]. For this reason, if one assumes an average roughness of 20 μm for the rectangular channels tested by Peng and Peterson [8], it is

possible to use the model in order to predict the laminar-to-turbulent transition. The results of the model are compared in Table 6 with the experimental data of Peng and Peterson [8]; the model predicts the same transition region for all the tested microchannel and this fact is in disagreement with the experimental results of [8]. Bearing in mind that the model proposed is valid for isothermal flows, the non-isothermal conditions and the absence of information about the real value of the surface roughness of the tested channels could partially explain the disagreement.

Nguyen *et al.* [25] investigated the flow friction and the forced convection through trapezoidal microchannels made by using anisotropic etching in silicon. The cross section is 500 μm deep and 1707 μm wide. The average relative roughness of the cross section is not measured. The experimental data revealed that the transition region extends in the range of 1000-1500 of the Reynolds number, but this result is obtained by heating the liquid flow, as in the work of Wang and Peng [6]. For this reason, also in this case, the comparison between the model and the data of Nguyen *et al.* [25] is not reliable. Nonetheless, it is possible to assume for the trapezoidal microchannels tested by Nguyen *et al.* [25] the same value of relative roughness measured by Harms *et al.* [22] for their microchannels, because they are obtained with the same technique (anisotropic etching). The results that can be obtained with the model are not so different with the experimental values found by Nguyen et al. [25], as it is possible to see in Table 6.

Pfund *et al.* [26] measured the pressure of water flowing along rectangular microchannels of 100-500 μm wide with an aspect ratio of 0.05. Transition to turbulence is observed at Re equal to 1450. The value of relative roughness is not measured. The microchannels tested by Pfund *et al.* are obtained with the same technique of the microchannels tested by Harms *et al.* [22]. For this reason, in order to test the model, a value of ε/D_h equal to 0.02 is assumed for these channels. Also in this case, the agreement with the predictions of the model is good.

It is possible to stress that the comparison between the model and the experimental data done good results but some aspect of the model have to be enhanced.

In order to improve the model it is important to make new experimental analyses in order to verify:

- the effect of the variation of the fluid thermophisical properties in heated microchannels on the laminar-to-turbulent transition; in this manner the constants comparing in Eqs.(9)-(10) could be correlated to the fluid temperature.
- the effect of the non-uniformity of the roughness on the wetted perimeter of the microchannels; this fact could make strong differences between the micro-channels and the classical rough commercial tube.

In conclusion, it was observed by many researcher that the laminar-to-transition in microchannels can occur at Reynolds numbers quite different with respect to the classical values obtained for non-circular channels by using the concept of hydraulic diameter. This fact is interpreted as a deviation from the classical theory. The experimental results available in literature show that the value of the transition Reynolds number is strongly influenced by the geometry of the cross-section and by the relative roughness of the microchannel. In this paper has been presented a model that permits to understand the role of these parameters. This model is based only on the results obtained by Jones and Obot for conventional sized channels. In the paper, a comparison between the model predictions and the experimental data obtained by different authors is presented in order to verify the reliability of this model for microchannels having an hydraulic diameter greater than 40 μm. The results of this comparison are encouraging and they have demonstrated that many experimental data on the laminar-to-turbulent flow transition in microchannels can be explained only by using the classical theory.

REFERENCES

1. W.J. Bowman and D. Maynes, A Review of Micro Heat Exchanger Flow Physics, Fabrication Methods and Application,, *Proc. ASME IMECE2001*, *HTD-24280*, 2001.
2. N.T. Obot, Toward a Better Understanding of Friction and Heat/Mass Transfer in Microchannels – A Literature Review, *Proc. Int. Conf. on Heat Transfer and Transport Phenomena in Microscale*, vol. 1, pp. 54-64, 2000.
3. P. Wu and W.A. Little, Measurement of Friction Factors for the Flow of Gases in Very Fine Channels used for Microminiature Joule-Thompson Refrigerators. *Cryogenics*, vol. 23, pp. 273-277, 1983.
4. P. Wu and W.A. Little, Measurement of Heat Transfer Characteristics of Gas Flow in Fine Channel Heat Exchangers used for Microminiature Refrigerators. *Cryogenics*, vol. 24, pp. 415-420, 1984.
5. S.B. Choi, R.F. Barron, R.O. Warrington, Liquid Flow and Heat Transfer in Microtubes, in *Micromechanical Sensors, Actuators and Systems*, ASME DSC, vol. 32, pp. 123-128, 1991.
6. B.X. Wang, X.F. Peng, Experimental Investigation on Liquid Forced-Convection Heat Transfer through Microchannels, *Int. J. Heat and Mass Transfer*, vol. 37, Suppl. 1, pp. 73-82, 1994
7. X.F. Peng, B.X. Wang, G.P. Peterson, H.B. Ma, Experimental Investigation of Heat Transfer in Flate Plates with Rectangular Microchannels, *Int. J. Heat and Mass Transfer*, vol. 38, pp. 127-137, 1995
8. X.F. Peng, G.P. Peterson, Forced Convection Heat Transfer of Single-Phase Binary Mixtures through Microchannels, *Exp. Thermal and Fluid Science*, vol. 12, pp. 98-104, 1996

9. G.P. Celata, M. Cumo, M. Guglielmi, G. Zummo, Experimental Investigation of Hydraulic and Single Phase Heat Transfer in 0.130 mm Capillary Tube, *Proc. Int. Conf. on Heat Transfer and Transport Phenomena in Microscale*, vol.1, pp. 108-113, 2000.
10. O.C. Jones, An Improvement in the Calculation of Turbulent Friction Factor in Rectangular Ducts, *Trans. ASME J. Fluids Eng.*, vol. 98, pp. 173-181, 1976.
11. N.T. Obot, Determination of Incompressible Flow Friction in Smooth Circular and Noncircular Passages. A Generalized Approach Including Validation of the Century Old Hydraulic Diameter Concept, *Trans. ASME J. Fluids Eng.*, vol. 110, pp. 431-440, 1988.
12. R.K. Shah and A.L. London, Laminar Flow Forced Convection in Ducts, *Adv. Heat Transfer*, Academic Press, New York, vol. 14, pp. 196, 1978
13. R. Sadasivam, R.M. Manglik, M.A. Jog, Fully Developed Forced Convection through Trapezoidal and Hexagonal Ducts, *Int. J. Heat and Mass Transfer*, vol. 42, pp. 4321-4331, 1999
14. M. Richter, P. Woias, D. Weiss, Microchannels for Applications in Liquid Dosing and Flow-Rate Measurement, *Sensors and Actuators A*, vol. 62, pp. 480-483, 1997
15. W. Urbanek, J.N. Zemel, H.H. Bau, An Investigation of the Temperature Dependence of Poiseuille Numbers in Microchannel Flow, *J. of Micromech. Microeng.*, vol. 3, pp. 206-209, 1993
16. V.K. Migay, Hydraulic Resistance of Triangular Channels in Laminar Flow, *Izv. Vyssh. Uchebn. Zaved. Energ.*, vol. 65, pp. 122-124, 1963
17. A. Takuto, K.M. Soo, I. Hiroshi, S. Kenjiro, An Experimental Investigation of Gaseous Flow Characteristics in Microchannels, *Proc. Int. Conf. on Heat Transfer and Transport Phenomena in Microscale*, vol.1, pp. 155-162, 2000.

18. N. Damean, P.P.L. Regtien, Poiseuille Number for the Fully Developed Laminar Flow Through Hexagonal Ducts Etched in <100> Silicon, *Sensors and Actuators A*, vol. 90, pp. 96-101, 2001

19. I. E. Idelchick, *Handbook of Hydraulic Resistance*, chap. 2, Hemisphere Publ. Co.,1986

20. R.E. Acosta, R.H. Muller, W.C. Tobias, Transport Processes in Narrow (Capillary) Channels. *AIChE Journal*, vol. 31, pp. 473-482, 1985.

21. F. Gui and R.P. Scaringe, Enhanced Heat Transfer in the Entrance Region of Microchannels, *Proc. of the 30th Intersociety Energy Conversion Eng. Conf.*, vol. 2, pp. 289-294, 1995

22. T.M. Harms, M.J. Kazmierczak, F.M. Gerner, Developing Convective Heat Transfer in Deep Rectangular Microchannels, *Int. J. Heat and Fluid Flow*, vol. 20, pp. 149-157, 1999.

23. L.S. Ding, H. Sun, X.L. Sheng, B.D. Lee, Measurement of Friction Factors for R134a and R12 through Microchannels, *Proc. Symposium on Energy Engineering in the 21st Century*, vol. 2, pp. 650-657, 2000.

24. P.X. Jiang, M.H. Fan, G.S. Si, Z.P. Ren, Thermal-Hydraulic Performance of Small Scale Micro-channel and Porous-Media Heat-Exchangers, *Int. J. Heat and Mass Transfer*, vol. 44, pp. 1039-1051, 2001

25. N.T. Nguyen, D. Bochnia, R. Kiehnscherrf, W. Dözel, Investigation of Forced Convection in Microfluid Systems, *Sensors and Actuators A*, vol. 55, pp. 49-55, 1996

26. D. Pfund, A. Shekarriz, A. Popescu, J.R. Welty, Pressure Drops Measurements in Microchannels, *ASME DSC- MEMS*, vol. 66, pp. 193-198, 1998

NOMENCLATURE

a, c	maximum and minimum channel width respectively, m
b	channel depth, m
C_R	geometry coefficient (= $(fRe)_{fd}\,\Gamma^*/2$)
D_h	hydraulic diameter, m (= $4\Omega / \Gamma$)
f	Fanning friction factor
p	pressure, Pa
Re	Reynolds number (=$\rho W D_h/\mu$)
V(.)	dimensionless fluid velocity
u(.)	fluid velocity, m/s
W	average velocity, m/s
β	channel aspect ratio (=c/a)
Φ_g^*	geometry function defined by Eq.(1)
γ	channel aspect ratio (=b/a)
Γ	cross-sectional perimeter, m
λ	molecular mean free path, m
μ	dynamic viscosity, kg/m s
ρ	density, kg/m^3
$\bar{\tau}_w$	mean wall shear stress, Pa
Ω	cross-sectional area, m^2

Table 1. The Poiseuille numbers for rectangular microchannels: comparison with the analytical values.

fRe_{fd}						
γ	0	0.05	0.1	0.2	0.3	0.4
Shan and London [12]	24	22.47701	21.16888	19.07050	17.51209	16.36810
Present results	24	22.477	21.169	19.071	17.512	16.368
γ	0.5	0.6	0.7	0.8	0.9	1
Shan and London [12]	15.54806	14.97996	14.60538	14.37780	14.26098	14.22708
Present results	15.548	14.980	14.605	14.378	14.261	14.227

Table 2. The Poiseuille numbers for microchannels etched on <100> silicon.

Trapezoidal			Double trapezoidal	
β	γ	fRe_{fd}	γ	fRe_{fd}
0	0	24	0	24
0.01	0.010	23.597	0.02	23.459
0.1	0.088	20.737	0.1	21.507
0.2	0.156	18.650	0.2	19.501
0.5	0.293	15.565	0.4	16.746
0.6	0.325	15.060	0.5	15.923
1	0.414	14.063	0.6	15.403
1.25	0.452	13.832	0.7	15.126
2	0.522	13.654	0.8	15.027
2.5	0.551	13.654	0.9	15.043
1/0.3	0.583	13.679	1	15.111
5	0.620	13.694	1.2	15.081
10	0.660	13.622	1.3	14.785
∞	0.707	13.308	1.414	14.055

Table 3. Comparison with the Poiseuille numbers quoted in the literature for triangular (γ=0.707) and trapezoidal KOH-etched microchannels.

fRe_{fd}				
γ	Present results	Takuto *et al.* [17]	Migay [16]	Urbanek *et al.* [15]
0.027	22.931	-	-	22.94
0.051	22.01	22.28	-	-
0.134	19.28	19.35	-	-
0.707	13.308	13.325	13.311	-

Table 4. Polynomial coefficients appearing in Eq. (8) for different cross-section of microchannels.

Cross-section	fRe_{fd}							
	g_0	g_1	g_2	g_3	g_4	g_5	γ range	Δ (%)
Rectangular	24	-32.549	46.777	-40.896	22.988	-6.0913	0 ÷1	+0.04
Trapezoidal	24	-42.267	64.272	-118.42	242.12	-178.79	0÷0.707	-0.14
Double Trapezoidal	24	-27.471	26.117	-6.6351	-0.2956	-0.5974	0÷1.414	0.05

Table 5. Critical Reynolds numbers for smooth (a) and rough (b) microchannels.

(a)

	Smooth microchannel (ε/D_h=0.007)								
	Rectangular			Trapezoidal			Double Trapezoidal		
γ	$Re_{c,0}$	$Re_{c,1}$	$Re_{c,2}$	$Re_{c,0}$	$Re_{c,1}$	$Re_{c,2}$	$Re_{c,0}$	$Re_{c,1}$	$Re_{c,2}$
0.05	2682	2814	4025	2628	2757	3944	2706	2839	4062
0.1	2525	2650	3790	2424	2543	3637	2565	2691	3850
0.2	2274	2386	3413	2087	2190	3133	2325	2440	3490
0.3	2089	2191	3135	1841	1931	2763	2138	2243	3209
0.4	1953	2049	2931	1689	1773	2536	1998	2096	2999
0.5	1855	1946	2784	1631	1712	2448	1900	1993	2851
0.6	1787	1875	2682	1631	1711	2448	1837	1927	2757
0.707	1739	1825	2611	1587	1665	2389	1802	1891	2704
0.8	1715	1799	2574				1792	1880	2689
0.9	1702	1785	2554				1795	1883	2694
1	1697	1781	2547				1803	1892	2706
1.1							1808	1897	2713
1.2							1798	1887	2699
1.3							1763	1850	2647
1.414							1677	1759	2516

(b)

	Rough microchannel (ε/D_h=0.02)								
	Rectangular			Trapezoidal			Double Trapezoidal		
γ	$Re_{c,0}$	$Re_{c,1}$	$Re_{c,2}$	$Re_{c,0}$	$Re_{c,1}$	$Re_{c,2}$	$Re_{c,0}$	$Re_{c,1}$	$Re_{c,2}$
0.05	1466	2507	3765	1437	2457	3690	1480	2530	3800
0.1	1381	2361	3546	1325	2265	3403	1403	2398	3602
0.2	1244	2126	3193	1141	1951	2931	1272	2174	3265
0.3	1142	1952	2933	1007	1721	2585	1169	1999	3002
0.4	1068	1825	2742	924	1579	2372	1093	1868	2805
0.5	1014	1734	2605	892	1525	2290	1039	1776	2667
0.6	977	1670	2509	892	1525	2290	1005	1717	2579
0.707	951	1626	2442	868	1483	2228	985	1684	2530
0.8	938	1603	2408				980	1675	2516
0.9	931	1591	2389				981	1678	2520
1	928	1586	2383				986	1685	2532
1.1							989	1690	2538
1.2							983	1681	2525
1.3							964	1648	2476
1.414							917	1567	2354

Table 6. Comparison with the main experimental data

on the laminar-to-turbulent flow transition quoted in literature.

.

	Cross-section	ε/D_h	γ	$Re_{c,0}$	$Re_{c,1}$	$Re_{c,2}$	Transition range of Re (exp. values)	Note
Wu and Little [3,4]	Trap.	Smooth	0.445	1653	1734	2480	1000-3000	Gas flow; isothermal flow
Acosta *et al*. [20]	Rect.	Smooth	0.019	2790	2928	4188	2770	Gas flow; isothermal flow
		Smooth	0.033	2739	2874	4111		
		Smooth	0.05	2682	2814	4025		
Nguyen *et al*. [25]	Trap.	0.02 (assumed)	0.292	1015	1734	2604	1000-1500	Liquid flow; non-isothermal flow
Gui and Scaringe [21]	Trap.	0.015	0.079	1527	2418	3584	1400	Liquid flow; non-isothermal flow
Pfund *et al*. [26]	Rect.	0.02 (assumed)	0.05	1466	2507	3765	1450	Liquid flow; isothermal flow
Jiang *et al*. [24]	Rect.	0.1	0.333	860	1596	2584	600-2800	Liquid flow;
Peng and Peterson [6]	Rect.	0.058	0.75	763	1435	2266	300-700	Liquid flow; non-isothermal flow average roughness (ε) assumed equal to 20 μm
		0.067	1	739	1389	2207	300-700	
		0.075	0.5	799	1499	2395	300-700	
		0.074	0.667	757	1420	2267	200-400	
		0.083	0.667	750	1403	2251	200-400	
		0.1	1	716	1329	2151	70-200	
		0.133	0.333	846	1547	2538	70-200	
		0.15	0.5	765	1389	2292	70-200	
Ding *et al*. [23]	Rect.	0.0075	1	1595	1767	2536	1500-1800	Liquid flow; isothermal flow
		Smooth	1	1697	1780	2546	1400-1500	
Harms *et al*. [22]	Rect.	Smooth	0.04	2716	2849	4076	1700	Liquid flow; non-isothermal flow
		0.02	0.244	1195	2044	3070	1510	

FIGURE CAPTIONS

Figure 1. Rectangular, trapezoidal and double-trapezoidal KOH-etched microchannels.

Figure 2. Geometry coefficient C_R of a KOH-etched trapezoidal microchannel as function of the aspect ratio.

Figure 3. Poiseuille numbers for a KOH-etched double-trapezoidal microchannel as function of the aspect ratio.

Figure 4. The geometry function Φ_g^* defined by Eq.(6) as function of the microchannels cross-section and aspect ratio.

Gian Luca Morini

Figure 1

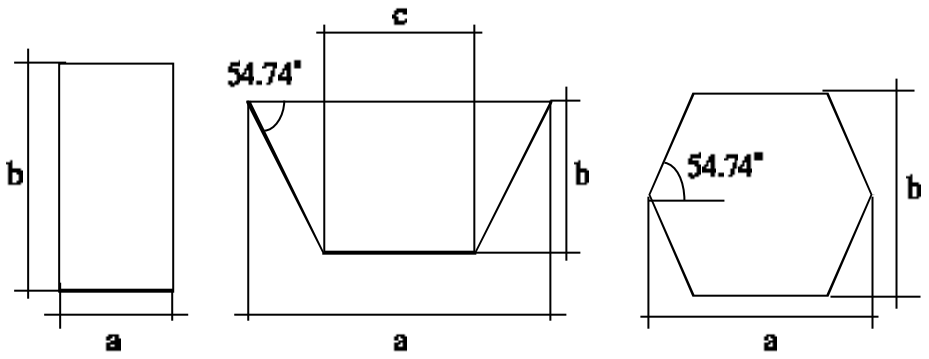

Figure 2

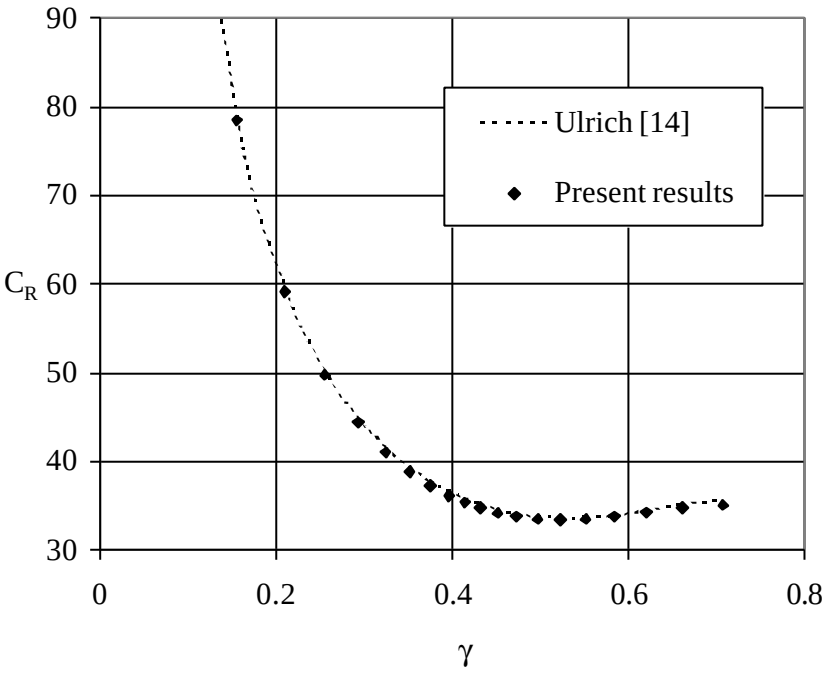

Figure 3

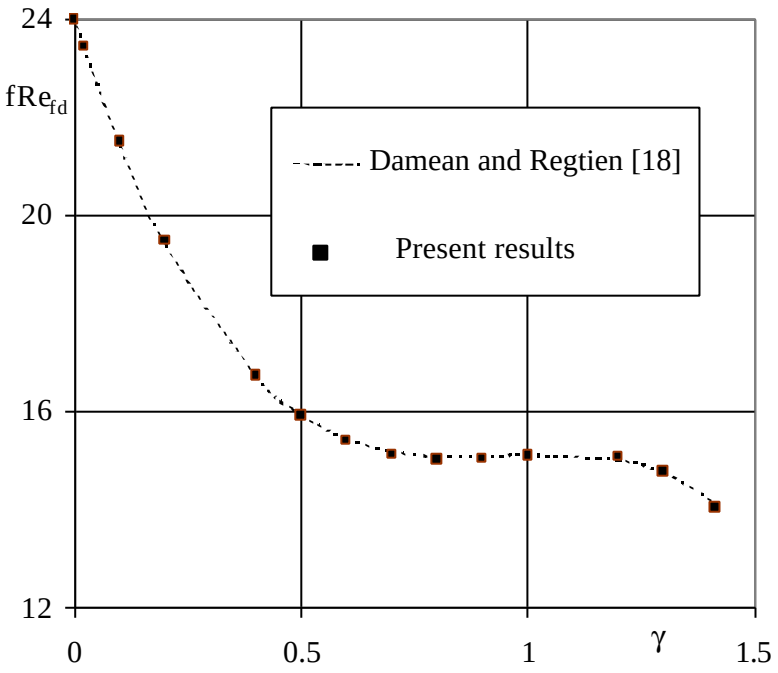
24
20
16
12
fRe$_{fd}$
0
0.5
1
1.5
γ
Damean and Regtien [18]
Present results

Gian Luca Morini

Figure 4